Frequency-, Temperature-, and Texture-dependent Dielectric Model for Frozen and Thawed Arctic Mineral Soils

V. L. Mironov[1], **I. P. Molostov**[1, 2], **Y. I. Luki**[1], **A. Y. Karavaysky**[1], **and S. V. Fomin**[1]

[1]Kirensky Institute of Physics, SB RAS, Russia
[2]Altai State University, Russia

Abstract— In this paper, a physically based dielectric model for frozen and thawed Arctic mineral soils is developed to account for moisture, dry density, temperature, texture of the soil and wave frequency. The model is based on the dielectric data measured for the three soils collected in the Yamal tundra, with clay content varying from 9.1% to 41.3%. Earlier developed the generalized refractive mixing dielectric model (GRMDM) was used as a theoretical basis for processing the measured data. In the frame of GRMDM the bound water and unbound water are identified as intrinsic parts of soil water. The maximum amount of bound water is considered to be a one of the basic major parameter of the proposed model. The dependence of this parameter on the soil temperature, and texture is derived, using dielectric data for the measured soils. In the measured frequency range 0.05 to 15 GHz, both the dipole and ionic interfacial (Maxwell-Wagner) dielectric relaxations were identified. These relaxation parameters for both parts of the soil water were determined as a function of temperature in the range −30 to 25°C, using the measured soil dielectric spectra and the multi-relaxation theoretical formula for them. Besides, the relaxation parameters were found to be independent on the soil texture. Electric conductivities for both parts of the soil water were determined as a function of temperature and clay content in the same temperature range, using the measured soil dielectric spectra and the theoretical formula for them. The error of the predicted values of the complex relative permittivity (CRP) of soils relative to the measured ones was evaluated through normalized root mean square error (nRMSE). The nRMSE appeared to be 5.5%, and 17.2% for the real and imaginary parts of the CRP, respectively.

1. INTRODUCTION

The products of the information technologies for obtaining top layer moisture of the thawed soils from the radiometry and radar remote sensing data have become available [1, 2] for using in the agricultural, weather forecast and climate change applications. Dielectric models of the soil are a key element linking the measured radiometry and radar data with the soil geophysical characteristics, such as soil moisture, and others [3, 4]. In the moisture retrieving algorithms of the most advanced microwave remote sensing instruments SMOS and SMAP the dielectric models developed by Dobson et al. [5] or Mironov et al. [6] are used, demonstrating acceptable accuracy on the global scale. Meanwhile, the researches on applying the SMOS and SMAP data for retrieving the thaw/freeze state [7] and frozen soil temperature [8] are now intensively carried out. But, ensuring these investigations dielectric models providing the relative complex permittivity of frozen and thawed mineral soils as a function of soil moisture, temperature, and texture are not available in the literature. Therefore the problem of developing an adequate dielectric model for frozen and thawed soils is of current importance.

In this paper, the temperature and texture dependent spectroscopic dielectric model for frozen and thawed mineral soils is developed for the MHz and GHz frequencies (0.05–15 GHz) in the temperature range from −30 to 25°C, for the soils with clay content varying up to 41.3%. The multi relaxation GRMDM, as it is outlined in [9], was applied as a theoretical basis to derive the proposed model parameters. The latter appeared to be the maximum amount of bound water, ohmic conductivities, as a function of temperature and clay content, and low and high frequency limits of dielectric constant, times of dielectric relaxations, as a functions of temperature. The obtained relaxation and conductivity parameters of the dielectric model are related, first, to bound water and unbound water, as distinct components of soil water, and second to the specific relaxation processes, which are dipole or ionic interfacial. The error of the predicted values of complex relative permittivity for the frozen and thawed soils was evaluated.

2. GENERALIZED REFRACTIVE MIXING DIELECTRIC MODEL

To develop the dielectric model we measured the three soils collected in Yamal peninsula, Russia. The data on texture and mineral compositions of the measured soils are shown in Table 1. Dielectric

measurements of frozen and thawed soils were carried out in the frequency range from 0.05 to 15 GHz for the soil moistures from zero to field capacity, with the temperature changing from 25°C to −30°C (cooling run).

Table 1. Texture and mineral composition of the measured group of soils.

No.	Soil Type	Soil Texture (%)			Mineral Composition (%)		
		Sand	Silt	Clay	Quartz	Feldspar	Plagioclase
1	Sandy loam	41.4	49.5	9.1	40	30	30
2	Silt loam	40.4	39.0	20.6	70	15	5–10
3	Silty clay	1.6	57.1	41.3	60	20-25	5

The procedures of soil samples preparation and dielectric measurement were the same as in [10]. The algorithm developed in [11] was applied to retrieve the spectra of the complex relative permittivity (CRP) of moist sample using the measured values of scattering matrix spectra for the measuring coaxial container.

For testing the used CRP measurement methodology and instrumentation, the special measurements were conducted for ethanol at temperature 20°C. Experimental data for the ethanol sample were fitted by Debye equations, and dielectric relaxation parameters were obtained. On the other hand, these Debye parameters are available for standard dielectric spectra given in [12]. The Debye parameters derived from our experiment with ethanol together with those taken from [12] are shown in Table 2. As seen from this table, the values of dielectric relaxation parameters obtained by us for ethanol deviate from values given in [12] not grater then by 7%, which proves the applicability of the methodology and instrumentation applied by us for dielectric measurement of soil. It should be noted that the deviations between Debye parameters obtained by us and standard once [12] can be caused by some water quantity in the measured ethanol sample.

Table 2. Dielectric relaxation parameters of ethanol at temperature 20°C.

Ethanol	ε_0	ε_∞	τ (ps)
Parameters from [12]	25.07	4.20	143.00
Parameters obtained by us	25.97 ± 0.12	4.42 ± 0.08	132.51 ± 1.45

2.1. The Model for Moisture Dependences of the Complex Refractive Indexes of Moist Soil

The generalized refractive mixing dielectric model (GRMDM) for frozen and thawed soil developed in this work is similar to that outlined in [9]. Compared to the model in [9] the proposed model was modified to ensure processing the measured soil dielectric data simultaneously for a number of soils with different textures. The introduced modification appeared possible due to the fact that the dielectric properties of such components of the measured soils, as bound water, unbound water, and soil solids, were found to be independent on soil texture.

The GRMDM formulas (2) and (3) in [9] describing the dependences of the soil reduced complex refractive indexes (CRIs), $(n_{sj}^* - 1)/\rho_d$, on moisture are reformulated as follows:

$$\frac{n_{sj}(m_g) - 1}{\rho_d} = \begin{cases} \frac{n_m - 1}{\rho_m} + \frac{n_b - 1}{\rho_b} m_g, & m_g < m_{g1j}; \\ \frac{n_{sj}(m_{g1j}) - 1}{\rho_d} + \frac{n_u - 1}{\rho_u}(m_g - m_{g1j}), & m_g \geq m_{g1j}; \end{cases} \tag{1}$$

$$\frac{\kappa_{sj}(m_g)}{\rho_d} = \begin{cases} \frac{\kappa_m}{\rho_m} + \frac{\kappa_b}{\rho_b} m_g, & m_g < m_{g1j}; \\ \frac{\kappa_{sj}(m_{g1j})}{\rho_d} + \frac{\kappa_u}{\rho_u}(m_g - m_{g1j}), & m_g \geq m_{g1j}; \end{cases} \tag{2}$$

where $n = \mathrm{Re}(\sqrt{\varepsilon})$ and $\kappa = \mathrm{Im}(\sqrt{\varepsilon})$ (ε — complex relative permittivity) are the refractive index (RI) and normalized attenuation coefficient (NAC), respectively, ρ is the density, m_g is the gravimetric moisture (ratio of the mass of soil water to that of the dry soil sample), and m_{g1j} is the maximum gravimetric fraction of bound water, so that the water in excess belongs to the unbound water component. The subscripts s, d, m, b, and u (which are related to n, κ, and ρ) refer to the moist soil, dry soil, solid (mineral) component of soil, bound water, and unbound water, respectively. Subscript j, which is related to n_s, κ_s, m_{g1}, refers to the number of soil samples as given in Table 1.

The densities of bound water in cases of frozen ($T < 0°\mathrm{C}$) and thawed ($T \geq 0°\mathrm{C}$) soil and unbound water in case of thawed soil are supposed to be the same as those for pure water ($\rho_b = 1\,\mathrm{g/cm^3}$). The density of unbound water in case of frozen soil is supposed to be the same as that for ice ($\rho_i = 0.917\,\mathrm{g/cm^3}$). The values $(n-1)/\rho$ and κ/ρ are referred to as the reduced RI and the reduced NAC.

The data collections consisting of measured reduced RIs and NACs for the three soils as a function of soil moisture at a fixed temperature and wave frequency, as shown in Fig. 1, were fitted by the piecewise linear functions (1) and (2). When fitting six functions (reduced RI(m_g) and NAC(m_g) for three types of soil) simultaneously the parameters $(n_m-1)/\rho_m$, $(n_b-1)/\rho_b$, $(n_u-1)/\rho_u$, κ_m/ρ_m, κ_b/ρ_b, and κ_u/ρ_u were derived as the same values for all three soils, but parameter m_{g1j} was individually derived for each soil of the measured group. As a result, there were derived 1) the maximum gravimetric fractions of bound water, m_{g11}, m_{g12}, and m_{g13}, pertaining to the soils 1, 2, and 3 (see Table 1); 2) the reduced RI and reduced NAC for the bound water, $(n_b-1)/\rho_b$, κ_b/ρ_b, unbound water, $(n_u-1)/\rho_u$, κ_u/ρ_u, and soil solids, $(n_m-1)/\rho_m$, κ_m/ρ_m.

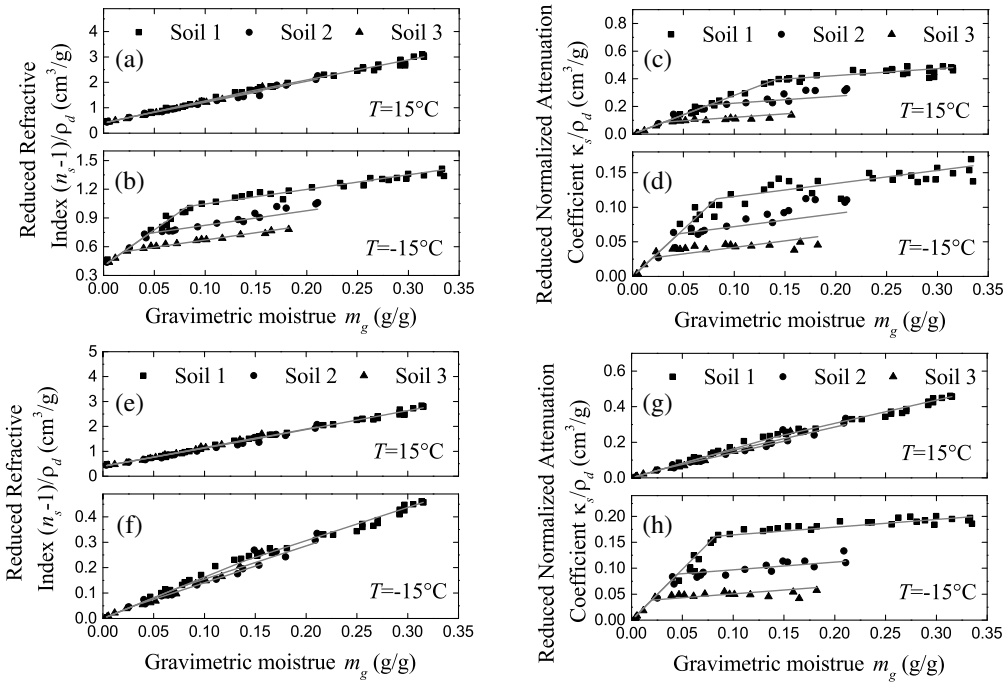

Figure 1. The reduced RI (a), (b), (e), (f) and reduced NAC (c), (d), (g), (h) of the measured soils (symbols) at wave frequency 0.5 GHz (a)–(d) and 5 GHz (e)–(h) as a function of gravimetric moisture. The solid lines indicate the fits of (1) and (2) to measured reduced RI and reduced NAC, respectively.

The above fitting procedure was performed for the measured data obtained at different temperatures (25, 20, 15, 10, 5, 0, −1, −2, −3, −4, −5, −10, −15, −20, −25, −30°C) and wave frequencies (400 points distributed with the same increment in the range from 0.05 to 15 GHz). The values of the reduced RI, $(n_m-1)/\rho_m$, and reduced NAC, κ_m/ρ_m, of soils solid component were averaged over wave frequency and temperature yielding the follows values:

$$\frac{n_m-1}{\rho_m} = 0.4; \quad \frac{\kappa_m}{\rho_m} = 0; \tag{3}$$

The values of the maximum gravimetric fractions of bound water m_{g1j} at a given temperature was averaged over the measured wave frequencies. As a result, the values of m_{g1j}, were derived as a function of both the temperature, T, and percentage of clay component, C, that is, $m_{g1j}(T,C)$. The data collection for $m_{g1j}(T,C)$, as shown in Fig. 2, was described by the following equations:

$$\begin{aligned}
&\text{when the soil in frozen state } (T < 0°\mathrm{C})\\
&m_{g1j}(T,C) = (0.0016 + 0.0017C) \times (1 + 1.2472\exp(T/7.1932));\\
&\text{when the soil in thawed state } (T \geq 0°\mathrm{C})\\
&m_{g1j}(T,C) = 0.0036C.
\end{aligned} \tag{4}$$

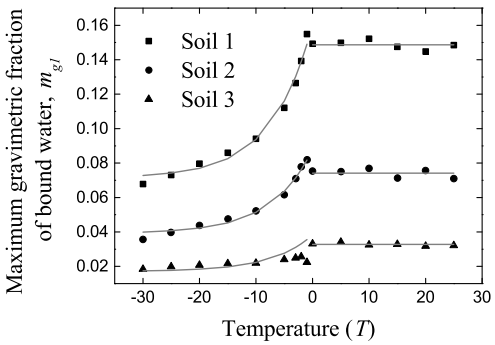

Figure 2. The maximum gravimetric fraction of bound as a function of gravimetric moisture. The solid lines indicate the fits (Equation (4)).

2.2. Frequency Dependencies of Dielectric Permittivity of Soil Water Components

The RI, n_p, and NAC, κ_p, with the subscript p, which indicate the bound water ($p = b$) and unbound water ($p = u$) soil water components, can be expressed through the dielectric constant (DC), ε'_p, and the loss factor (LF), ε''_p, as follows:

$$n_p = \sqrt{\sqrt{(\varepsilon'_p)^2 + (\varepsilon''_p)^2} + (\varepsilon'_p)^2}/\sqrt{2}; \quad \kappa_p = \sqrt{\sqrt{(\varepsilon'_p)^2 + (\varepsilon''_p)^2} - (\varepsilon'_p)^2}/\sqrt{2}. \tag{5}$$

Similar to [9], we express the DC and the LF of the components of soil water in (5) using the equations for the Debye and Maxwell-Wagner multiple relaxations [13] of non-conductive liquids, which account for only bias electric currents:

$$\varepsilon'_p = \frac{\varepsilon_{0pL} - \varepsilon_{0pM}}{1 + (2\pi f \tau_{pL})^2} + \frac{\varepsilon_{0pM} - \varepsilon_{0pH}}{1 + (2\pi f \tau_{pM})^2} + \frac{\varepsilon_{0pH} - \varepsilon_{\infty pH}}{1 + (2\pi f \tau_{pH})^2} + \varepsilon_{\infty pH}; \tag{6}$$

$$\varepsilon''_p = \frac{\varepsilon_{0pL} - \varepsilon_{0pM}}{1 + (2\pi f \tau_{pL})^2}(2\pi f \tau_{pL}) + \frac{\varepsilon_{0pM} - \varepsilon_{0pH}}{1 + (2\pi f \tau_{pM})^2}(2\pi f \tau_{pM}) + \frac{\varepsilon_{0pH} - \varepsilon_{\infty pH}}{1 + (2\pi f \tau_{pH})^2}(2\pi f \tau_{pH}); \tag{7}$$

where f is the wave frequency, ε_{0pL}, ε_{0pM}, and ε_{0pH} are the low frequency limits of the dielectric constants, and $\varepsilon_{\infty pH}$ is the high frequency limit for the dielectric constant of the dipole relaxation. The subscripts H, M, and L refer to the high frequency, middle frequency, and low frequency relaxations, respectively. The high frequency relaxation is a dipole relaxation, whereas the middle frequency and low frequency relaxations are assumed to be the ionic interfacial (Maxwell-Wagner) relaxations. The parameters τ_{pL}, τ_{pM}, and τ_{pH} are the respective relaxation times. All of these parameters should be related to the bound water ($p = b$) or unbound water ($p = u$) components of the soil water. In the case of the bound water, a three relaxations Equations (6), (7) are used. In the case of the unbound water, single relaxation equations are applied, which follows from (6), (7) with $\varepsilon_{0uL} = \varepsilon_{0uM} = \varepsilon_{0uH}$.

The LF, ε''_p, that are determined by Equation (7) do not include a term that accounts for the ohmic conductivity of the soil water components. Nevertheless, keeping in mind that only the bias currents account for the DC of moist soil, ε'_p, we can express this value in the form

$$\varepsilon'_{sj} = n^2_{sj} - \kappa^2_{sj}; \tag{8}$$

where Equations (1), (2) are used to calculate the RI, n_s, and NAC, κ_s. At the same time, the LF of moist soil, ε''_p, can be represented as the sum of two terms

$$\varepsilon''_{sj} = 2n_{sj}\kappa_{sj} + \sigma_s/(2\pi f \varepsilon_r); \tag{9}$$

where σ_s is the specific conductivity of the soil sample, and $\varepsilon_r = 8.854\,\mathrm{pF/m}$ is the dielectric constant of the free space.

As in [9], it is suggested that the ohmic conductivity of the sample is equal to a sum of conductivities arising due to the presents of 1) bound water, and 2) unbound water. Then suggesting

that each of those is equal to the conductivity of the respective water component weighted by their relative volumetric fractions, we can represent similar to formula (8) in [9] the LF of the moist soils in the following form:

$$\varepsilon''_{sj} = \begin{cases} 2n_{sj}\kappa_{sj} + \rho_d(\sigma_{bj}m_g/\rho_b)/(2\pi f\varepsilon_r), & m_g < m_{g1j}; \\ 2n_{sj}\kappa_{sj} + \rho_d(\sigma_{bj}m_{g1j}/\rho_b + \sigma_{uj}(m_g - m_{g1})/\rho_u)/(2\pi f\varepsilon_r), & m_g \geq m_{g1j}; \end{cases} \quad (10)$$

where the values σ_{bj} and σ_{uj} are the specific ohmic conductivities for the bound water and unbound water, respectively.

Equations (1)–(10) show that the DC and LF spectra at a given soil temperature as a function of the input variables (dry soil density, ρ_d, gravimetric soil moisture, m_g, and wave frequency, f) can be calculated using the following set of parameters: $(n_m - 1)/\rho_m$, κ_m/ρ_m, m_{g1j}, ε_{0pQ}, $\varepsilon_{\infty pH}$, τ_{pQ}, σ_{pj}, which are related to i) the bound water ($p = b$) and unbound water ($p = u$) components of the soil water and ii) the high frequency ($Q = H$), middle frequency ($Q = M$), and low frequency ($Q = L$) relaxations of the soil water components. The dielectric model parameters ε_{0pQ}, $\varepsilon_{\infty pH}$, τ_{pQ}, σ_{pj} can be derived as in [9] by fitting the spectra for the DC and LF of moist soil samples measured at different moistures and temperatures using formula (8) and (10) as theoretical model. In contrast to [9] the spectra of samples belonging to different types of soils were fitted simultaneously. So what appear to be the same for the individual three soils the values of parameters ε_{0pQ}, $\varepsilon_{\infty pH}$, τ_{pQ} are determined common to all samples. While the values of parameter σ_{pj} were found to be different for the soils with individual clay contents, independently for each sample. As an example, several patterns for DC and LF spectra of soils are shown in Fig. 3. The theoretical spectra for the DC calculated with the parameters resulting from fitting, ε_{0pQ}, $\varepsilon_{\infty pH}$, τ_{pQ}, σ_{pj}, $(p = b, u;\ Q = H, M, L)$ are also shown by solid lines in Fig. 3, and they demonstrate good correlation with the measured data. As a result of fitting of DC, and LF spectra measured at the temperatures (25, 20, 15, 10, 5, 0, −1, −2, −3, −4, −5, −10, −15, −20, −25, −30°C) the experimental dependences of all the above parameters on the temperature were obtained, $\varepsilon_{0pQ}(T)$, $\varepsilon_{\infty pH}(T)$, $\tau_{pQ}(T)$, $\sigma_{pj}(T)$, similar to those shown in Figs. 3, 4, 5 which are given in [9].

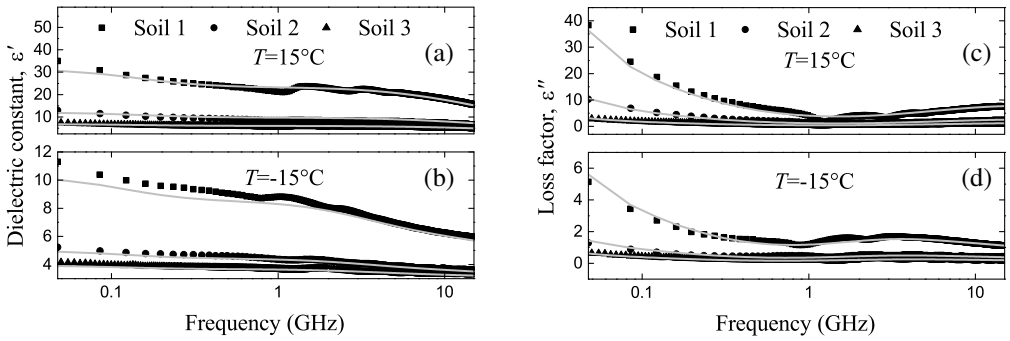

Figure 3. Spectra of (a), (b) DC, ε'_s, and (c), (d) LF, ε''_s, corresponding to the measured data (symbols) and respective fits (lines), with ε'_s, and ε''_s being fitted by the theoretical models expressed by the set of equations i) (1)-(8) and ii) (1)-(7) and (10), respectively. Moisture of samples are equal to 0.23, 0.09, 0.07 for samples 1, 2 and 3 in (a) and (c), respectively, and 0.25, 0.13, 0.07 for samples 1, 2 and 3 in (b) and (d), respectively. Density of samples are equal 1.59, 1.43, 1.49 for samples 1, 2 and 3 in (a) and (c), respectively, and 1.6, 1.44, 1,49 for samples 1, 2 and 3 in (b) and (d), respectively.

2.3. Parameters of the Temperature-Dependent GRMDM

We suggest that the temperature dependences for low and high frequency limits of dielectric constants follow the equation that was obtained in [14] with the use of the Clausius-Mossotti law [15]:

$$\varepsilon_{qpQ} = \frac{1 + 2\exp[F_{qpQ}(T_{s\varepsilon qpQ}) - \beta_{\nu qpQ}(T - T_{s\varepsilon qpQ})]}{1 - \exp[F_{qpQ}(T_{s\varepsilon qpQ} - \beta_{\nu qpQ}(T - T_{s\varepsilon qpQ})]}; \quad F_{qpQ}(T) = \ln\left[\frac{\varepsilon_{qpQ}(T) - 1}{\varepsilon_{qpQ}(T) + 2}\right] \quad (11)$$

where ε_{qpQ} and $\beta_{\nu qpQ}$ stand for the low ($q = 0$) and high ($q = \infty$) frequency limit dielectric constants and the volumetric expansion coefficients, respectively, that are related to the bound water ($p = b$) and unbound water ($p = u$) components of the soil water. The subscript Q represents the low ($Q = L$), middle ($Q = M$), and high ($Q = H$) frequency relaxations of the soil water

components, and $T_{s\varepsilon qpQ}$ represents the starting temperature, which can be any value from the measured temperature intervals. The values of $\beta_{\nu qpQ}$ and $\varepsilon_{qpQ}(T_{s\varepsilon qpQ})$ can be determined by fitting the theoretical model (11) to the previously obtained in Subsection 2.2 experimental temperature dependences $\varepsilon_{0pQ}(T)$ $(p = b, u;\ Q = H, M, L)$, as it was done in [9] (see Fig. 3 of [9]). The values of $\beta_{\nu qpQ}$, $T_{s\varepsilon qpQ}$, and $\varepsilon_{qpQ}(T_{s\varepsilon qpQ})$ derived from the fitting are given in Table 3.

Table 3. TD GRMDM parameters for all forms of soil water in the temperature range $-30°\text{C} \le T \le 25°\text{C}$.

Temperature		$T < 0°\text{C}$				$T \ge 0°\text{C}$			
Soil water component		Bound water $(p = b)$			Unbound water $(p = u)$	Bound water $(p = b)$			Unbound water $(p = u)$
Relaxations		High $(Q = H)$	Middle $(Q = M)$	Low $(Q = L)$	High $(Q = H)$	High $(Q = H)$	Middle $(Q = M)$	Low $(Q = L)$	High $(Q = H)$
Parameters	Units								
$\varepsilon_{0pQ}(T_{s\varepsilon 0pQ})$	-	23.91	64.18	97.69	5.54	52.49	81.29	166.91	78.18
$T_{s\varepsilon 0pQ}$	°C	−20	−20	−20	−20	20	20	20	20
$\beta_{\nu 0pQ}$	1/K $\times 10^{-3}$	−2.18	−0.34	−0.63	−2.06	−1.14	−0.01	−0.22	0.10
$\Delta H_{pQ}/R$	K	184.0	2484.1	47.6	4567.4	1826.9	86.0	454.8	2147.0
$\Delta S_{pQ}/R$	-	−3.33	3.89	−8.80	12.57	2.71	−4.79	−7.31	3.35
$\varepsilon_{\infty pQ}(T_{s\varepsilon\infty pQ})$	-	12.34			4.31	7.25			4.31
$T_{s\varepsilon\infty pQ}$	°C	−20			−20	20			20
$\beta_{\nu\infty pQ}$	1/K $\times 10^{-3}$	2.9			0	7.9			0

As in [14] the temperature dependences for the relaxation times can be described by the Eyring equation [15]:

$$\ln\left(\frac{kT_K}{h}\tau_{pQ}\right) = \frac{\Delta H_{pQ}}{R}\frac{1}{T_K} - \frac{\Delta S_{pQ}}{R}; \tag{12}$$

where h is the Plank constant $(6.624 \times 10^{-34}$ Js), k is the Boltzmann constant $(1.38 \times 10^{-23}$ JK$^{-1})$, ΔH_{pQ} is the activation energy of the relaxation process, R is the universal gas constant $(8.314 \times 10^3$ JK^{-1}kmol$^{-1})$, ΔS_{pQ} is the entropy of activation, and T_K is the temperature in Kelvin. The ratios $\Delta H_{pQ}/R$ and $\Delta S_{pQ}/R$, which are proportional to the activation energy and the entropy of activation, respectively, can be determined by fitting the theoretical model (12) to the previously obtained in Subsection 2.2 experimental temperature dependences $\ln(kT_K\tau_{pQ}(T)/h)$ $(p = b, u;\ Q = H, M, L)$, as it was done in [9] (see Fig. 4 of [9]). The values of parameters $\Delta H_{pQ}/R$ and $\Delta S_{pQ}/R$ derived from fitting are given in Table 3 and can be used to calculate the relaxation time using Equation (12).

Finally, we suggest that the ohmic conductivity, σ_{pj}, has a linear dependence with temperature, which is characteristic for ionic solutions:

$$\sigma_{pj} = \sigma_{pj}(T_{s\sigma p}) + \beta_{\sigma pj}(T - T_{s\sigma p}); \tag{13}$$

where $\beta_{\sigma pj}$ is the derivative of conductivity with respect to temperature, which is also referred to as the conductivity temperature coefficient, and $\sigma_{pj}(T_{s\sigma p})$ is the value of conductivity at an arbitrary starting temperature, $T_{s\sigma p}$, that is taken from the measured range. Subscript j refers to the number of individual soil samples from as given in Table 1. The values of $\sigma_{pj}(T_{s\sigma p})$ and $\beta_{\sigma pj}$ can be determined by fitting the theoretical model (13) to the experimental temperature dependences previously obtained in Subsection 2.2 $\sigma_{pj}(T)$ $(p = u, i)$, as it was done in [9] (see Fig. 5 of [9]). Clay content dependences of parameters $\beta_{\sigma pj}$ and $\sigma_{pj}(T_{s\sigma p})$ was fitted by linier function. As a result, obtaining the following formula:
when the soil in frozen state $(T < 0°\text{C})$

$$\begin{aligned}
&\beta_{\sigma bj} = (0.05C + 1.03)10^{-3}\,(\text{S/m})/\text{K}; \quad \sigma_{bj}(T_{s\sigma b}) = (0.6C + 14.07)10^{-3}\,\text{S/m};\\
&\beta_{\sigma uj} = (0.04C + 0.17)10^{-3}\,(\text{S/m})/\text{K}; \quad \sigma_{uj}(T_{s\sigma u}) = (0.35C + 2.05)10^{-3}\,\text{S/m};\\
&T_{s\sigma b} = T_{s\sigma u} = -20°\text{C};
\end{aligned} \tag{14}$$

when the soil in thawed state ($T \geq 0°\mathrm{C}$)

$$\begin{aligned} &\beta_{\sigma bj} = (0.11C + 1.38)10^{-3}\,(\mathrm{S/m})/\mathrm{K}; \quad \sigma_{bj}(T_{s\sigma b}) = (4.6C + 55.01)10^{-3}\,\mathrm{S/m}; \\ &\beta_{\sigma uj} = (0.11C + 0.15)10^{-3}\,(\mathrm{S/m})/\mathrm{K}; \quad \sigma_{uj}(T_{s\sigma u}) = (5.94C + 17.6)10^{-3}\,\mathrm{S/m}; \\ &T_{s\sigma b} = T_{s\sigma u} = 20°\mathrm{C}. \end{aligned} \tag{15}$$

As a result of the analyses conducted in this section, proposed model can be defined by the following steps, which form the algorithm procedure.

1. The temperature, T, must be assigned.
2. The values of the Debye parameters, including the high and low frequency limits of dielectric constant and relaxation time, for all types of soil water are calculated with Equations (11)–(12) and the data in Table 3.
3. Once the values of $\varepsilon_{qpQ}(T)$ and $\tau_{pQ}(T)$ are known, the values of the DC, $\varepsilon'_p(f,T)$, and the LF $\varepsilon''_p(f,T)$ for all components of the soil water can be calculated as a function of frequency at a given temperature using the Equations (6) and (7), respectively.
4. The values of $\varepsilon'_p(f,T)$ and $\varepsilon''_p(f,T)$ are translated to the RI, n_p, and NAC, κ_p, for all of the components of the soil water using the Equation (5).
5. The gravimetric soil moisture, m_g, and the dry soil bulk density, ρ_d, must be assigned, and Equations (1)–(4) are applied to calculate the soil RI, $n_{sj}(\rho_d, m_g, f, T)$, and the NAC, $\kappa_{sj}(\rho_d, m_g, f, T)$, accounting for bias currents.
6. Finally, the values of $n_{sj}(\rho_d, m_g, f, T)$ and $\kappa_{sj}(\rho_d, m_g, f, T)$ are translated to the soil DC, $\varepsilon'_{sj}(\rho_d, m_g, f, T)$, and the LF, $\varepsilon''_{sj}(\rho_d, m_g, f, T)$, with Equation (8) and Equation (10), respectively, using the values of the specific conductivities calculated by (13)–(15).

2.4. Evaluation of the Model

To quantify the statistical errors of the present dielectric model we estimated the values of determination coefficients (R^2) and the values of normalized root mean square error (nRMSE). R^2 and nRMSE were estimated with the following formulas:

$$R^2 = 1 - \sum_{i=0}^{N}(x_i - y_i)^2 \Bigg/ \sum_{i=0}^{N}(x_i - \bar{x})^2; \quad \mathrm{nRMSE} = \sqrt{\sum_{i=0}^{N}(x_i - y_i)^2/n} \cdot \frac{100\%}{\bar{x}} \tag{16}$$

where x_i, y_i, $\bar{x}$ are measured values, predicted values, and the average measured values, respectively; N is number of measurements. Evaluation of the proposed dielectric model yielded the values of nRMSE 5.5% and 17.2% for the DC and LF, respectively. While the values of R^2 were found to be 0.994 and 0.989 for the DC and LF, respectively.

3. CONCLUSION

A temperature-, frequency- and texture-dependent dielectric model was developed for frozen mineral soils on the bases of dielectric data measured in the frequency range from 0.05 to 15 GHz for the three soils with clay content 9.1%, 20.6%, and 41.3% in the temperature range from 25°C to −30°C in the range of soil moistures varying from 0 to the field capacity for the dry densities of soil samples limited in the range from 1.3 to 1.8 g/cm^3. The model provides the CRPs of the frozen and thawed mineral soils as a function of dry soil density, moisture, texture (clay content), frequency and temperature. The estimated values of nRMSE were found to be on the same order as the dielectric measurement errors themself.

Ultimately, the dielectric model suggested in this study forms the basis for developing data processing algorithms in the cases of thawed and frozen soils for the modern remote sensing missions, such as AQUA, GCOM-W, SMOS, SMAP, RADARSAT, and ALOS PALSAR, as well as for perspective P-band sensors. In addition, it will facilitate the applications of the GPR and TDR instruments, which operate in the megahertz band, make impossible to interpret the results of in situ measurements of the active permafrost layer.

ACKNOWLEDGMENT

Present research was supported in the frame of project No. 16-45-242162 in the corporative program of the Russian foundation for basic research and Krasnoyarsk region government foundation for science and technology. It was also supported by the RAS Presidium Program "Arctika", 2015–2017 and program II.12.1. of the SB RAS basic researches.

REFERENCES

1. NRT L2 Soil Moisture Neural Network (SMOS.MIRAS.NRT_L2SM_NN) [Online]. Available: https://earth.esa.int/web/guest/data-access/latest-data-products.
2. SMAP L2 Radiometer Half-Orbit 36 km EASE-Grid Soil Moisture, Version 3 [Online]. Available: https://nsidc.org/data/SPL2SMP/versions/3.
3. Mialon, A., P. Richaume, D. Leroux, et al., "Comparison of dobson and mironov dielectric models in the SMOS soil moisture retrieval algorithm," *IEEE Trans. Geosci. Remote Sens.*, Vol. 53, No. 6, 3084–3094, 2015.
4. Chan, S. K., R. Bindlish, P. E. ONeill, et al., "Assessment of the SMAP passive soil moisture product," *IEEE Trans. Geosci. Remote Sens.*, Vol. 54, No. 8, 4994–5007, 2016.
5. Dobson, M. C., F. T. Ulaby, M. T. Hallikainen, and M. A. El-Rayes, "Microwave dielectric behavior of wet soil-Part II: Dielectric mixing models," *IEEE Trans. Geosci. Remote Sens.*, Vol. 23, No. 1, 35–46, 1985.
6. Mironov, V. L., L. G. Kosolapova, and S. V. Fomin, "Physically and mineralogically based spectroscopic dielectric model for moist soils," *IEEE Trans. Geosci. Remote Sens.*, Vol. 47, No. 7, 2059–2070, 2009.
7. Roy, A., A. Royer, C. Derksen, et al., "Evaluation of spaceborne L-band radiometer measurements for terrestrial freeze/thaw retrievals in Canada," *IEEE J. Sel. Appl. Earth Observ.*, Vol. 8, No. 9, 4442–4459, 2015.
8. Muzalevskiy, K. V. and Z. Ruzicka, "Retrieving soil temperature at a test site on the yamal peninsula based on the SMOS brightness temperature observations," *IEEE J. Sel. Appl. Earth Observ.*, Vol. 9, No. 6, 2468–2477, 2016.
9. Mironov, V. L. and I. V. Savin, "A temperature-dependent multi-relaxation spectroscopic dielectric model for thawed and frozen organic soil at 0.05–15 GHz," *Physics and Chemistry of the Earth, Parts A/B/C*, Vols. 83–84, 57–64, 2015.
10. Mironov, V. L., Y. H. Kerr, L. G. Kosolapova, et al., "A Temperature-dependent dielectric model for thawed and frozen organic soil at 1.4 GHz," *IEEE J. Sel. Appl. Earth Observ.*, Vol. 8, No. 9, 4470–4477, 2015.
11. Mironov, V. L., I. P. Molostov, Yu. I. Lukin, and A. Yu. Karavaisky, "Method of retrieving permittivity from S_{12} element of the waveguide scattering matrix," *Proceedings of SIBCON*, 1–3, Krasnoyarsk, Russia, September 2013.
12. Buckley, F. and A. A. Maryott, "Tables of dielectric dispersion data for pure liquids and dilute solutions," US Dept. of Commerce, National Bureau of Standards, Washington, 1958.
13. Kremer, F. and A. Schonhals, *Broadband Dielectric Spectroscopy*, 1st Edition, Springer, Germany, 2003.
14. Mironov, V. L., R. D. De Roo, and I. V. Savin, "Temperature-dependable microwave dielectric model for an arctic soil," *IEEE Trans. Geosci. Remote Sens.*, Vol. 48, No. 6, 2544–2556, 2010.
15. Dorf, R. C., *Electrical Engineering Handbook*, 2nd Edition, CRC Press, Boca Raton, FL, 1997.